Biosensors and Bioelectronics 24 (2008) 836–841

Contents lists available at ScienceDirect

Biosensors and Bioelectronics

journal homepage: www.elsevier.com/locate/bios

Shear acoustic wave biosensor for detecting DNA intrinsic viscosity and conformation: A study with QCM-D

Achilleas Tsortos[a], George Papadakis[a], Electra Gizeli[a,b,*]

[a] Institute of Molecular Biology and Biotechnology, FO.R.T.H, Heraklion 71110, Greece
[b] Department of Biology, University of Crete, Heraklion 71409, Greece

ARTICLE INFO

Article history:
Received 16 April 2008
Received in revised form 18 June 2008
Accepted 4 July 2008
Available online 15 July 2008

Keywords:
DNA conformation
Intrinsic viscosity
QCM-D
Acoustic biosensor
Model

ABSTRACT

Direct biosensors are devices operating by monitoring the amount of surface-bound analyte. In this work a new approach is presented where a label-free acoustic biosensor, based on a QCM-D device, and solution viscosity theory, are used to study DNA intrinsic viscosity. The latter is quantitatively related to the DNA conformation and specifically the molecule's shape and size, in a manner that is independent of the amount of bound DNA mass. It is shown that acoustic measurements can clearly distinguish between ds-DNA of same shape (straight rod) but various sizes (from 20 to 198 bp (base pairs)) and same mass and size (90 bp) but various shapes ("straight", "bent", "triangle"). These results are discussed in the broader context of "coil" and sphere-like molecules detected on surfaces.

A mathematical formula is presented relating the length of straight, surface-protruding DNA to the acoustic ratio $\Delta D/\Delta f$. The development of real-time rapid techniques for the characterization of DNA intrinsic curvature as well as DNA conformational changes upon interaction with proteins is of significance to analytical biotechnology due to the large number of DNA sequences and potential DNA bending proteins involved in genome analysis and drug screening.

1. Introduction

During the last decade acoustic wave devices have received considerable attention and have emerged as a significant alternative to optical biosensors. Two factors have contributed to the popularity of acoustic wave biosensors; first an increase in our understanding of how shear acoustic waves interact with (bio)mass deposited on the device surface, together with the development of mathematical models describing such complex systems. Secondly, the fact that shear acoustic wave devices have become commercially available, therefore, the technology is now accessible to the non-acoustic specialist's laboratory.

Of the various types of acoustic devices reported in literature, the Quartz Crystal Microbalance (QCM) and the Love Surface Acoustic Wave (SAW) devices are the most common shear acoustic wave devices used in liquid-phase sensing applications. QCM's response to the deposition of a thin layer of rigid mass (Δm) is governed by the Sauerbrey equation, derived for a crystal operating in air that relates frequency change (Δf) to Δm in a linear way (Sauerbrey, 1959). The introduction of an experimental set-up that allows, in addition to Δf, measurement of the dissipation (ΔD) of the acoustic energy associated with the deposition of a viscoelastic layer, significantly increased the information gained from QCM experiments (Ozeki et al., 2007; Rodahl et al., 1995, 1997). Furthermore, a new mathematical treatment based on the Voigt model of a viscoelastic layer was applied to derive information on the film thickness (d_f), effective density (ρ_f), shear viscosity (η_f) and elastic modulus (μ_f) of the adlayer (Voinova et al., 1999). The combined measurement of Δf and ΔD together with the Voigt model were applied to the acoustic characterization of the viscoelasticity of protein layers (Hook et al., 2001a) and single stranded and hybridized DNA films (Larsson et al., 2003; Su et al., 2005). Furthermore, the ratio between ΔD and Δf, i.e., the measured energy dissipation per surface-coupled unit mass, can be used as a qualitative fingerprint of the studied biofilms and derive information related to the structure of the layer (i.e., relative rigidity, its water content, etc.) (Hook et al., 2001a; Rodahl et al., 1997). A basic feature of the Voigt model is that the deposited layer is treated as a homogeneous viscoelastic film therefore, mass sensed by the sensor is thought of as the mass of macromolecules plus "trapped" water. Furthermore, combination of the Surface Plasmon Resonance (SPR) with QCM-D measurements and

* Corresponding author at: Institute of Molecular Biology and Biotechnology, FO.R.T.H, Vassilika Vouton, Heraklion 71110, Greece. Tel.: +30 2810 394373; fax: +30 2810 391101.
E-mail address: gizeli@imbb.forth.gr (E. Gizeli).

0956-5663/$ – see front matter © 2008 Elsevier B.V. All rights reserved.
doi:10.1016/j.bios.2008.07.006

the Voigt model was shown to improve the precision by which the viscoelastic components of the probed film, i.e., η_f and μ_f can be separated and quantified (Larsson et al., 2003; Peh et al., 2007).

On the other hand, the response of the Love wave sensor, a waveguide configuration with high sensitivity to surface perturbations (Du et al., 1997; Gizeli, 1997) consists of the measurement of the phase Ph (i.e., frequency) and amplitude A (i.e., energy) of the acoustic wave. Similarly to the QCM-D, changes in mass (Δm) and viscosity or viscoelastic properties of the interface can be detected via the changes ΔPh and ΔA, respectively. The drawback of the Love wave sensor is the lack of a simple mathematical model that would relate Δm to ΔPh. Perturbation theory has been used to derive a dispersive equation describing the interaction of an acoustic wave in a general layered waveguide structure covered with a thin film overlay which perturbs the mechanical boundary conditions (Herrmann et al., 1999; Kovacs and Venema, 1992; McMullan et al., 2000; McHale et al., 2002). An alternative approach based on a semi-empirical method was also used to model and calculate phase change as a function of deposited mass (Saha et al., 2003).

In this work a new physical explanation, supported by a mathematical treatment, is described. The approach is based on the fact that biomolecules such as DNA anchored to the device surface behave as discrete molecules, rather than a homogeneous viscoelastic film, and can, thus, be modeled using classical solution viscosity theory (Cantor and Schimmel, 1980; Tanford, 1961). In a previous work (Tsortos et al., 2008) we showed that the above theory can be used to characterize DNA molecules with respect to their size and shape in combination with acoustic measurements obtained with a Love wave device. In the current work the model is applied to the QCM-D device and shown to hold equally well. Changes in the measured ratio $\Delta D/\Delta f$ parallel changes in the intrinsic viscosity of various DNA molecules and allow us to discriminate between the binding of DNA of similar shape but various sizes; in addition, DNA of same mass but different shape can clearly be distinguished in a quantitative manner. This model is the first attempt to provide a unified theory which is applicable to both types of shear acoustic wave sensors, i.e., the QCM-D and Love wave device.

2. Experimental

2.1. Acoustic device

A QCM (Q-Sense D300, Sweden) acoustic device was used; the operating frequency for the results reported here is the 35 MHz overtone. For the sake of comparison with the Love wave device (Tsortos et al., 2008), experiments were carried out on QCM sensor surfaces that were treated in the following way. A 0.4-μm thick waveguide layer of PMMA was deposited on the surface of the acoustic device by spin-coating the device at 4000 rpm with a 8 % (w/w) solution of medium molecular weight poly(methyl methacrylate) in 2-ethoxyethylacetate (Aldrich). The PMMA-covered devices were heated to 195 °C for 2 h to promote solvent evaporation. A 20-nm gold layer was deposited on top of it by sputter-coating with a Bal-Tec SCD 050 sputter-coater (Liechtenstein). The gold layer was etched immediately prior to the acoustic experiments to ensure a clean surface. Devices were re-used after etching to clean off adsorbed samples; a new layer of gold (20 nm thick) was added by sputter-coating. Nevertheless, no significant differences were noticed when the chips were used as received from the supplier without the PMMA coating.

2.2. DNA design and preparation

Biotinylated double-stranded DNA (ds-DNA) of various lengths (20, 50, 90, 132, 167, 198, 270, 395 and 1724 base pairs) where prepared using standard annealing and PCR amplification techniques (Tsortos et al., 2008). In addition, another 90-mer oligonucleotide was designed based on sequences from previous studies that are known to create different degrees of (intrinsic) curvature to the molecule. The sequences of the two 90 bp oligos are the following:

"Straight" (out of phase): 5′-tcttgctggc gttcgcgacg aaacgcgcgc gcaaaaaacg cgcgcgcaaa aaacgcgcgc gcaaaaaacg cgttgcaggc catgctgtcc-3′.

"Bent" (in phase): 5′-tcttgctggc gttcgcgacg cgaaaaaacg cgaaaaaacg cgaaaaaacg cgaaaaaacg cgaaaaaacg cgttgcaggc catgctgtcc-3′.

The "bent", i.e., a bent at half-length DNA chain, was prepared having biotin at either one or both ends.

Curvature analysis of the two 90 bp products was performed using CURVE (http://www.lfd.uci.edu/~gohlke/curve/) and GSVIEW software and verified by mobility differences on a 12% polyacrylamide gel under native conditions (Papadakis, 2008).

2.3. Real-time acoustic detection of neutravidin and DNA binding

A continuous flow of Tris buffer (50 mM Tris pH 7.5, 10 mM $MgCl_2$ and 10 mM KCl) was pumped over the surface of the gold-coated devices at a flow rate of 20 μl/min. The signal was allowed to equilibrate prior to the first addition and all samples were added in the same buffer. Neutravidin (Pierce) was added at a concentration of 10 μg/ml for 12 min, long enough to saturate the sensor surface with a protein layer. After a buffer rinse, DNA samples were added in Tris buffer at a range of concentrations varying between 1.2 and 14 μg/ml. Glycerol (Biomol, Germany) and IgG protein (Vector, USA) where also measured.

3. Acoustic model

The correlation between acoustic measurements and the viscosity of the interface layer has been documented for the QCM-D sensor (Voinova et al., 1999). Changes in energy dissipation, measured by the QCM as ΔD, reflect changes in solution viscosity η at the substrate/liquid interface and within the sensed volume; consequently, changes in ΔD should follow closely viscosity changes resulting from the addition of molecules such as DNA at the interface. In addition, frequency changes Δf, are correlated to the amount of deposited mass on the device surface (Hook et al., 2001a). Classical analysis of the viscosity of macromolecule solutions provides a well-tested theory where the solution viscosity η can be correlated to the solvent viscosity η_0 and the solute (i.e., DNA) concentration C and intrinsic viscosity $[\eta]$ (Box 1 , Eq. (1)). Furthermore, theory predicts that, for non-interacting particles, viscosity should be independent of the concentration of the solute molecules and should depend solely on the intrinsic viscosity of the solute particles (Box 1, Eq. (2)).

Based on the above, i.e., the assumptions that ΔD corresponds to viscosity η or specific viscosity η_{sp} (since η_0 is just a constant for the buffer solution) and Δf is equivalent to the macromolecule (surface) concentration C^{surf}, acoustic measurements can be directly related to the dissolved (non-interacting) particle's intrinsic viscosity, as indicated by Eq. (3), Box 1. In practice, and if the theory holds true, this would indicate that, for a given DNA solution applied to the device surface, the detected ratio $\Delta D/\Delta f$ should be constant and independent of the solute molecules concentration or surface density (Box 1, B).

Box 1

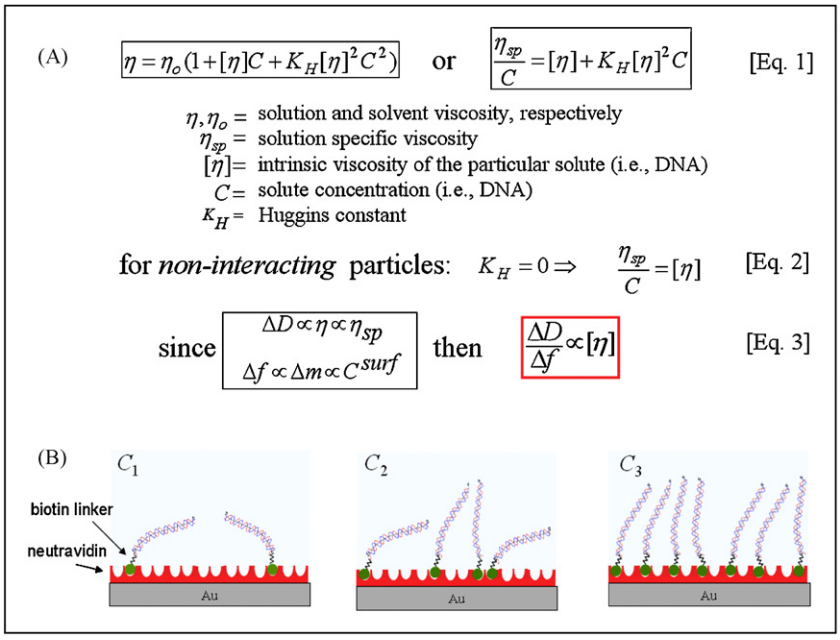

(A) Correlation of classical macromolecule solution viscosity theory to acoustic measurements based on the assumptions that ΔD corresponds to viscosity η_{sp}, and Δf is equivalent to the macromolecule (surface)concentration C^{surf}. (B) Schematic representation of device/liquid interface for different DNA surface concentrations ($C_3 > C_2 > C_1$). Eq. (3) predicts that for the same DNA molecule, the acoustic ratio $\Delta D/\Delta f$ detected during DNA binding should be constant, independent of surface coverage and proportional to the molecule's intrinsic viscosity.

In addition, since the above theory reveals that the acoustic ratio is proportional to the intrinsic viscosity of each DNA molecule ($\Delta D/\Delta f \propto [\eta]$), then it should be possible to apply directly well-known equations that correlate intrinsic viscosity to the macromolecule's size and shape. In the case of straight, rod-shaped molecules, the Mark–Houwink equation (Box 2, Eq. (4)) describes the relationship between intrinsic viscosity and the molecular weight (MW) and shape (α) of a macromolecule in a particular solvent; for straight DNA molecules, the MW can be directly related to the molecule's length (L) while the coefficient α can be calculated for each DNA length (Box 2, Eq. (5)), (Cantor and Schimmel, 1980). Again, this would imply that, if the proposed theory holds true, plotting $\Delta D/\Delta f$ versus L^{α} should give a straight line. Note that for calculating the coefficient α, the shape factor ν for stiff, straight DNA can be approximated to that of a prolate ellipsoid with major and minor axis determined by the length (L) and radius (b), respectively, of the DNA molecules.

The shape factors (ν) used in the case of "straight"-rod DNA molecules can not be applied to correlate acoustic measurements to the intrinsic viscosity of "bent"- or "triangle"-type DNA and more sophisticated mathematical models are required. "Bent" rods (as compared to a "straight" rod of diameter D and length L) have been modeled as having two rod-like arms of lengths L_1 and L_2 joined end-to-end at an angle χ. The two components have the same diameter and the total length is L, where $L = L_1 + L_2$. Their hydrodynamic behavior has been extensively studied theoretically using a "bead" model (Garcia de la Torre and Bloomfield, 1978, 1981). Calculations based on these models can produce values for the ratio $[\eta]_{bent}/[\eta]_{straight}$ which depend on the angle χ. Since in our approach this ratio is equivalent to the acoustic ratio $(\Delta D/\Delta f)_{bent}/(\Delta D/\Delta f)_{straight}$ the critical test would be to compare the two. The same bead model was also used for the "triangle" configuration calculations. A detailed description of the above treatment can be found elsewhere (Tsortos et al., 2008).

4. Results

Double-stranded DNA molecules were bound to a neutravidin modified device surface by using biotin attached to the end of the DNA molecule through a hinge of 11 carbon atoms. Loading of the samples in a flow-through format allowed the continuous additions of DNA samples and Tris buffer in an alternating way. Fig. 1 shows the real-time binding of different length biotinylated-DNA onto the neutravidin modified device surface; the DNA attachment to the device surface was specific since control experiments performed with non-biotinylated DNA gave no detectable signal. From this figure the change in dissipation and frequency can be calculated as a function of DNA length. The same was done for different concentrations of each particular DNA length. Fig. 2 shows the measured ΔD versus Δf values for various concentrations of four of these different DNA molecules (20, 90, 198 and 1724 bp). It can be seen that the acoustic ratio (indicated by the slope of each line) is independent of the loaded DNA concentration, (resulting to different extents of surface coverage), and is different for each one of the four DNA samples. This observation holds true for all the straight DNA molecules applied in this work (data not shown). A striking feature of the system is that the measured ratio of each DNA molecule was found to be independent of the device history; adding different DNA samples during the same experiment in random order had no effect in the measured values, suggesting that this measurement reflects only intrinsic properties of each molecule. For comparison, data obtained for various concentrations of glycerol and protein solutions is also included in Fig. 2.

Box 2

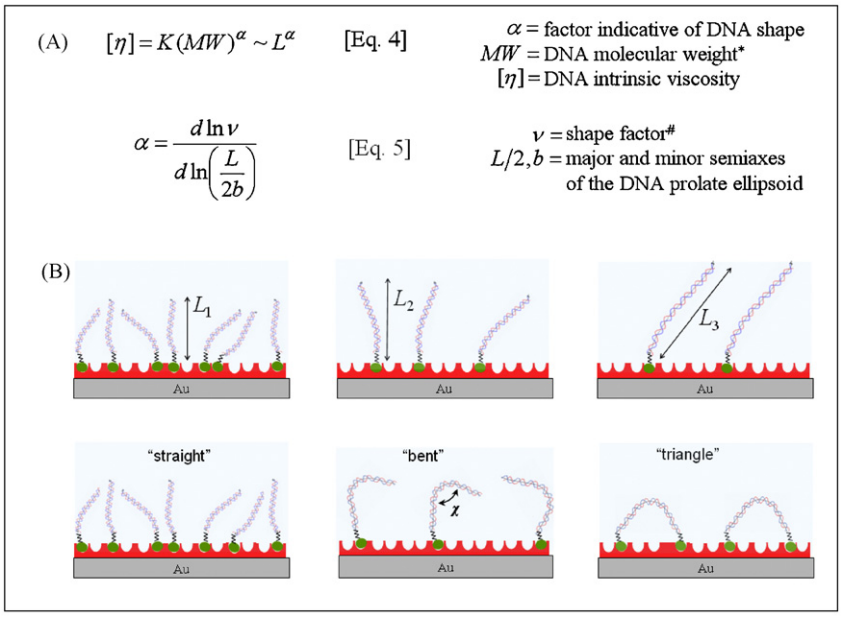

(A) The Mark–Houwink relation [Eq. (4)] is used to model straight, rod-shaped ds-DNA; this equation correlates the intrinsic viscosity with the molecular weight and shape of a macromolecule in a particular solvent. *For DNA, a rod of constant diameter and density, the MW is linearly related to its length L. #The shape factor is calculated by approximating the shape of stiff DNA molecules with that of a prolate ellipsoid. (B) Schematic representation of the solid/liquid interface when DNA molecules of various lengths $L_3 > L_2 > L_1$ and same shape, or various shapes but same length are used. The bending angle χ is also shown.

Furthermore, plotting $\Delta D/\Delta f$ versus length, for all DNA molecules used in this work, gives a sigmoidal line (Fig. 3). In order to correlate the acoustic ratio obtained during the binding of "straight" DNA molecules to the device surface to the molecules' length L and shape α, as predicted by Eqs. (3) and (4) (Boxes 1 and 2, respectively), $\Delta D/\Delta f$ was also plotted against L^{α} (Fig. 3, inset).

5. Discussion

In order to correlate real-time acoustic measurements derived with the QCM-D with solution viscosity theory presented in Boxes 1 and 2, acoustic data obtained during DNA binding to the sensor surface were expressed as the ratio of dissipation change over frequency change ($\Delta D/\Delta f$); this ratio is a measure of the energy dissipation per coupled unit mass and, based on theoretical predictions, should provide insight on viscosity changes occurring at the sensor/liquid interface as a result of DNA binding. First, the validity of the hypothesis that $\Delta D/\Delta f$ should be related to the intrinsic viscosity of each DNA molecule and, thus, be constant, different and characteristic for each DNA molecule as well as independent of DNA concentration or surface coverage was confirmed experimentally by obtaining a straight line when plotting ΔD against Δf (Fig. 2); note that ΔD and Δf were detected dur-

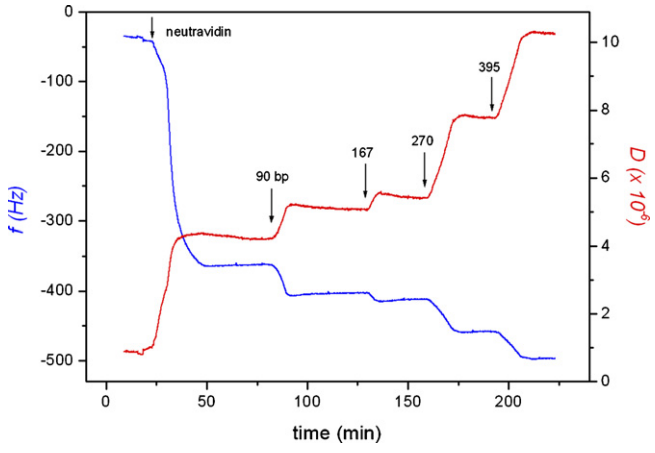

Fig. 1. Real-time binding curves for frequency (f) and dissipation (D) during the application of neutravidin, followed by DNA samples, for the 35 MHz overtone of the QCM-D acoustic device.

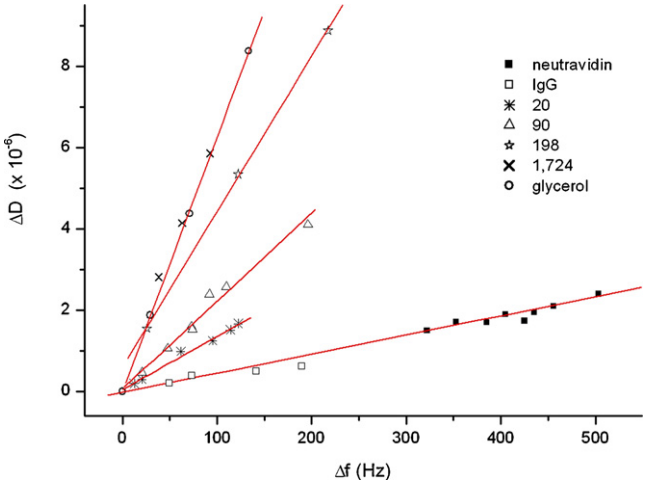

Fig. 2. Plot of the acoustic signal ΔD vs. Δf for various concentrations of applied analyte (i.e., various % surface coverage) for neutravidin, IgG, glycerol and four ds-DNA lengths.

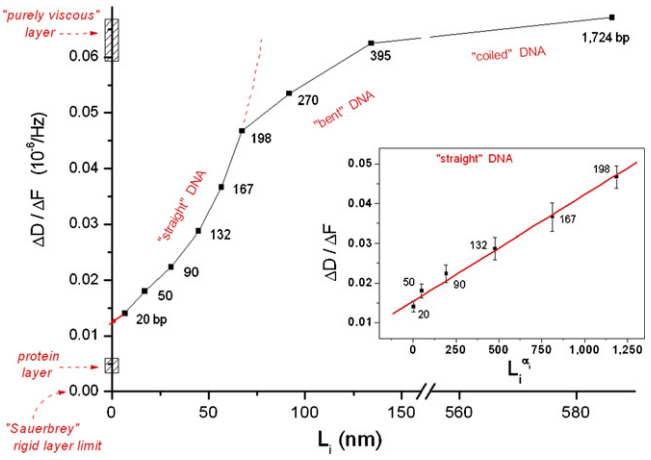

Fig. 3. Plot of the ratio $\Delta D/\Delta f$ vs. contour length L of straight (20–198 bp) and bent or coiled (270–1724 bp) DNA molecules. The inset shows how, for the straight DNA, the curve relationship is turned into linear ($R = 0.991$) when plotted vs. L^{α} (α values are calculated for each length separately and are the following: 0.728, 1.377, 1.538, 1.621, 1.658 and 1.681 for 20, 50, 90, 132, 167 and 198 bp, respectively). The Y-axis is equivalent to (η_{sp}/C^{surf}) or $[\eta]$, (see model).

ing the loading of various concentrations of DNA solutions to the device surface. Since Eq. (3) was derived for non-interacting particles, this would also imply that surface-attached DNA molecules do not interact with each other. Looking at the surface chemistry reveals that DNA chains are kept apart and translational or complete rotational motions are prohibited since the molecules are anchored on the protein substrate; note that in this arrangement there is one chain per neutravidin molecule spaced 6–7 nm apart (Larsson et al., 2003). Their movement is expected to be a surface-driven oscillation at various tilt angles from the normal (Levicky et al., 1998; Moiseev et al., 2006; Wong and Pettitt, 2004), depending on surface coverage. In addition, DNA chains, carrying negative charges at pH 7.5, would also exhibit electrostatic repulsions among each other and with the negatively charged surface (neutravidin's pI = 6.3). Given the above, one would conclude that, in this case, the probability of having lateral hydrodynamic interactions between neighboring surface-attached DNA molecules is in this case, indeed, minimal.

Fig. 3 shows that the acoustic ratio can be used as a fingerprint to distinguish between the binding of different "straight" DNA molecules with 20–198 bp (lengths of 6.8–67.3 nm, assuming 0.34 nm per base pair). This observation suggests that all the above DNA molecules are within the sensor's penetration depth (δ), which is 95 nm for pure water, and are, thus, fully probed by the device. Furthermore, assuming that viscosity theory predicts well enough the behavior of the acoustic system, the curved line (first part of the sigmoidal) obtained experimentally when the acoustic ratio is plotted against the DNA length should be turned into a straight line if the ratio is plotted again, this time versus L^{α} (Box 2, Eq. (4)). As can be seen in Fig. 3 (inset), an excellent fit is obtained validating the above approach. Note that the coefficient α was calculated for each DNA molecule assuming that DNA has the shape of a prolate ellipsoid (Box 2, Eq. (4)). The persistence length of the ds-DNA used in this work is between 50 and 80 nm (Levicky et al., 1998; Lu et al., 2002); in that respect all DNA, up to 198 bp, applied on the device surface may be safely considered as short stiff rods with a major ellipsoid axis determined by each molecule's length and a minor axis identical for all molecules and equal to the DNA diameter (2 nm).

Interestingly, DNA with 270, 395 and 1724 bp (with corresponding contour lengths L of 91.8, 134.3 and 586.2 nm) deviates from the extrapolated (dots, Fig. 3) position, fast approaching plateau values of $\Delta D/\Delta f$. For these molecules L is greater than the persistence length and are thus expected not to be straight rods any more. Progressively, they acquire bents and finally become more coil-like. This means that the requirement for prolate structures (Box 2, Eqs. (4) and (5)) is no longer fulfilled; the theory can not be applied as is and an extension of it is under investigation. As can be seen (Figs. 2 and 3) the $\Delta D/\Delta f$ value for the longest DNA is identical to that of glycerol. Glycerol is a "pure viscous" case solution and the measured value $\Delta f/\Delta D \approx 16 \pm 2(\mathrm{Hz}/10^{-6})$ is that predicted by theory (Kanazawa and Gordon, 1985; Ozeki et al., 2007; Rodahl et al., 1995) at the frequency of 35 MHz, i.e., 17.5(Hz/10^{-6}). While glycerol appears at the top of the graph (Figs. 2 and 3) the lower "boundary" is of course, the Sauerbrey "rigid film" limit where $\Delta D/\Delta f = 0$ (Ozeki et al., 2007; Hook et al., 1998). Proteins (neutravidin and IgG) are approaching this limit but are not quite there: $\Delta D/\Delta f \approx 0.0048(10^{-6}/\mathrm{Hz})$, (Larsson et al., 2003; Ozeki et al., 2007). A very short ($L \to 0$), surface protruding DNA rod gives a value (extrapolated Y-axis intercept) of $\Delta D/\Delta f \approx 0.0144(10^{-6}/\mathrm{Hz})$, shown to be equivalent to a flat-lying chain (Furusawa et al., 2006; Tsortos et al., 2008). This value is about three times that of a protein "compact layer" case, as shown in Figs. 2 and 3 and measured before with a Love wave device (Tsortos et al., 2008).

Turning to the intrinsically "bent" DNA now we see that good agreement between the theoretically calculated ratio $[\eta]_{bent}/[\eta]_{straight}$ and the experimentally measured one $(\Delta D/\Delta f)_{bent}/(\Delta D/\Delta f)_{straight}$ would require an angle χ of $114 \pm 9^{\circ}$. This value is clearly a very reasonable one as can be seen in Box 2 where the molecule is realistically drawn based on DNA-curvature analysis using the GSVIEW software. This result compares favorably with $105 \pm 6^{\circ}$ obtained from a Love wave device (Tsortos et al., 2008). For the case of the 90 bp DNA molecule placed in a "triangle" conformation (anchored on the surface by two biotin hinges instead of one) using an approximation for this shape within the context of the "bead" model again, the corresponding theoretical ratio $[\eta]_{triangle}/[\eta]_{straight}$ is in the range of 0.74–0.48; the experimentally measured value for the ratio $(\Delta D/\Delta f)_{triangle}/(\Delta D/\Delta f)_{straight}$ of 0.56 ± 0.05 falls again correctly in the predicted range.

The new theoretical approach and experimental verification presented here reveals that acoustic measurements can be correlated to the intrinsic properties of DNA molecules attached to the device surface. This approach is different to existing models (Voinova et al., 1999) where DNA bound through biotin/streptavidin at a QCM device surface is treated as a viscoelastic layer in order to derive average bulk properties of the whole layer, i.e., viscosity, elastic modulus, effective density and thickness. The viscoelastic model assumes that liquid trapped between the molecules is measured as additional "acoustic" mass. Based on the above, in hybridization studies carried out on a QCM-D device surface, the higher energy dissipation per coupled unit mass observed for double stranded DNA compared to the single stranded one was attributed to further water entrapment (Aung et al., 2008; Hook et al., 2001b; Larsson et al., 2003; Ozeki et al., 2007; Stengel et al., 2005; Su et al., 2005). Although one could see the validity of the viscoelastic model in the case of a densely packed protein layer adsorbed on the device surface, this is less obvious in the case of surface-attached DNA molecules. First, the amount of sensed trapped water between adjacent molecules for low DNA surface coverage would be nearly zero; secondly, for higher DNA surface densities, the amount of trapped water would be expected to depend on and increase with DNA surface coverage. Experimental data presented both in this work and in similar studies carried out with a Love wave shear acoustic wave device, clearly show that the acoustic ratio is independent of surface coverage. A "coil"-to-"stiff rod" type of structural transition, suggested by our model, could possibly explain the higher $\Delta D/\Delta f$

observed for ds-DNA, compared to single stranded molecules, since a coil has a smaller $[\eta]$ value than a straight rod. On the other hand, frequency changes measured with a TSM acoustic wave device were related to the DNA concentration-dependent viscosity change within the acoustic wave decay length region δ (Su and Thompson, 1995). Using classical viscosity theory the authors successfully predicted the value 1.8 for the Mark–Houwink exponent "α", suggestive of a stiff rod conformation for their hybridised strands.

6. Conclusions

In this work, a new theory is presented which correlates acoustic wave measurements to the intrinsic viscosity and subsequently, conformation of surface-attached DNA molecules. This theory, already presented for shear acoustic waves propagating in a Love wave device, is shown to hold true for the QCM-D system. Acoustic ratio measurements during the binding of DNA molecules on the sensor surface can be used to discriminate between DNA of various sizes and shapes independently of the amount of surface bound quantities. Systematic variation of the "straight" DNA length gave an excellent agreement between acoustic measurements and macromolecule solution viscosity theory for "straight" DNA molecules with a rod-type shape. "Bent" and "triangle" DNA molecules confirmed that the theory works remarkably well in describing systems of various shapes. Plots like the one shown in Fig. 3 (inset) can be used as a calibration curve. An empirical equation, fitting the data from this work and valid for up to ~ 200 bp DNA, is:

$$\frac{\Delta D}{\Delta f} = 1.4 + 7 \times 10^{-3} \times L + 6 \times 10^{-4} \times L^2 \quad (6)$$

where $\Delta D/\Delta f$ is measured at 35 MHz in units of $(10^{-8}/\text{Hz})$ and L in nm. For example, using this equation for a 34-bp DNA sample we get the same value calculated from published data, i.e., 1.6×10^{-8}/Hz (Aung et al., 2008).

Other research areas, where the concepts of viscosity have been employed, are in the areas of measuring viscosity using a QCM sensor (Saluja and Kalonia, 2004), as well as in microfluidics/microchip devices (Lee and Tripathi, 2005). The importance of the shape of DNA and DNA complexes has long been recognized in pharmaceutical practice and similar approaches in its measurements, i.e., through viscosity, have also been described (Sun et al., 2003). An area of greatest interest is the detection of protein-driven DNA bending (Luscombe et al., 2000) in order to characterize DNA binding proteins such as transcription factors. In general, this work suggests that acoustic biosensors can be developed into a rapid method for the detection of DNA intrinsic conformation and DNA conformational changes; the latter leads to the unique possibility of screening for potential drugs that affect transcription and regulation through protein-driven bending.

Acknowledgement

The authors would like to acknowledge the Human Frontier Science Program (HFSP) for financially supporting this work.

References

Aung, K.M.M., Ho, X., Su, X., 2008. Sens. Actuators B: Chem. 131, 371–378.
Cantor, C.R., Schimmel, P.R., 1980. Biophysical Chemistry. Part II. Freeman, San Francisco.
Du, J., Harding, G.L., Collings, P.R., Dencher, P.R., 1997. Sens. Actuators A: Phys. 60, 54–61.
Garcia de la Torre, J., Bloomfield, V., 1978. Biopolymers 17, 1605–1627.
Garcia de la Torre, J., Bloomfield, V., 1981. Q. Rev. Biophys. 14, 81–139.
Gizeli, E., 1997. Smart Mater. Struct. 6, 700–706.
Herrmann, F., Hahn, D., Büttgenbach, S., 1999. Sens. Actuators A: Phys. 78, 99–107.
Hook, F., Kasemo, B., Nylander, T., Fant, C., Sott, K., Elwing, H., 2001a. Anal. Chem. 73, 5796–5804.
Hook, F., Ray, A., Norden, B., Kasemo, B., 2001b. Langmuir 17, 8305–8312.
Hook, F., Rodahl, M., Brzezinski, B., Kasemo, B., 1998. Langmuir 14, 729–734.
Kanazawa, K.K., Gordon, J.G., 1985. Anal. Chim. Acta 175, 99–105.
Kovacs, G., Venema, A., 1992. Appl. Phys. Lett. 61, 639–641.
Larsson, C., Rodahl, M., Hook, F., 2003. Anal. Chem. 75, 5080–5087.
Lee, J., Tripathi, A., 2005. Anal. Chem. 77, 7137–7147.
Levicky, R., Herne, T.M., Tarlov, M.J., Satija, S.K., 1998. J. Am. Chem. Soc. 120, 9787–9792.
Lu, Y., Weers, B., Stelllwagen, N.C., 2002. Biopolymers 61, 261–275.
Luscombe, N.M., Austin, S.E., Berman, H.M., Thornton, J.M., 2000. Genome Biol. 1, 1–37.
McMullan, C., Mehta, H., Gizeli, E., Lowe, C.R., 2000. J. Phys. D: Appl. Phys. 33, 3053–3059.
Moiseev, L., Unlu, M.S., Swan, A.K., Goldberg, B.B., Cantor, C.R., 2006. Proc. Natl. Acad. Sci. U.S.A. 103, 2623–2628.
McHale, G., Newton, M.I., Martin, F., 2002. J. Appl. Phys. 91, 9701–9710.
Ozeki, T., Morita, M., Yoshimine, H., Furusawa, H., Okahata, Y., 2007. Anal. Chem. 79, 79–88.
Furusawa, H., Ozeki, T., Okahata, Y., 2006. Nucl. Acids Symp. Series 50, 321–322.
Papadakis, G., 2008. Ph.D. Thesis, University of Crete.
Peh, W.Y.X., Reimhult, E., Teh, H.F., Thomsen, J.S., Su, X., 2007. Biophys. J. 92, 4415–4423.
Rodahl, M., Hook, F., Brzezinski, P., Kasemo, B., 1995. Rev. Sci. Instrum. 66, 3924–3930.
Rodahl, M., Hook, F., Fredriksson, C., Keller, C.A., Krozer, A., Brzezinski, P., Voinova, M., Kasemo, B., 1997. Faraday Discuss. 107, 229–246.
Saha, K., Bender, F., Rasmusson, A., Gizeli, E., 2003. Langmuir 19, 1304–1311.
Saluja, A., Kalonia, D.S., 2004. AAPS PharmSciTech. 5 (3) (Article number 47).
Sauerbrey, G., 1959. Z. Phys. 155, 206–222.
Stengel, G., Hook, F., Knoll, W., 2005. Anal. Chem. 77, 3709–3714.
Su, H., Thompson, M., 1995. Biosens. Bioelectron. 10, 329–340.
Su, X., Wu, Y.J., Knoll, W., 2005. Biosens. Bioelectron. 21, 719–726.
Sun, Y., Li, X., Duzgunes, N., Takaoka, Y., Ohi, S., Hirota, S., 2003. Biophys. J. 85, 1223–1232.
Tanford, C., 1961. Physical Chemistry of Macromolecules. Wiley, New York.
Tsortos, A., Papadakis, G., Mitsakakis, K., Melzak, K.A., Gizeli, E., 2008. Biophys. J. 94, 2706–2715.
Voinova, M.V., Rodahl, M., Jonson, M., Kasemo, B., 1999. Phys. Scripta 59, 391–396.
Wong, K.Y., Pettitt, B.M., 2004. Biopolymers 73, 570–578.